Proceedings of the 28th IEEE
EMBS Annual International Conference
New York City, USA, Aug 30-Sept 3, 2006

A MIMO channel approach for characterizing electrode-tissue interface in long-term chronic microelectrode array recordings

Karim G. Oweiss, *Member, IEEE*

Abstract—**Characterizing the encapsulation layer caused by glial scar formation surrounding microelectrode arrays in chronic implants has been the subject of extensive research. Typically, an equivalent circuit model is used to characterize the reactive tissue response by nonlinearly fitting the electrical impedance spectroscopy (EIS) data. This model assumes a time invariant adjacent layer of encapsulation tissue to have the same structure on every electrode site. In this paper, an alternative approach is proposed based on modeling the encapsulation layer as a time varying communication channel. The channel is characterized by a Multi-input Multi-output (MIMO) transfer function with time varying coefficients. This model circumvents spatial resolution limitations of existing EIS equivalent circuit models. It further allows capturing the observed changes in neural signal quality over time. We show that "equalizing" the channel using this model can yield a substantial improvement in signal quality. With tendency towards high-density electrode arrays for cortical implantation, the proposed model is better suited to equalize the fading channel and interpret the recorded signals with higher accuracy. We also show conceptually how patterned waveforms can periodically be used to probe the channel if adverse effects can be avoided. This can potentially improve the channel estimator performance, particularly when cell migration occurs.**

I. Introduction

Chronic implants in the nervous system are among the ultimate goals to permit treatment of a large number of neurological disorders and enable better understanding of the underlying function of the nervous system at the cellular level. Recording properties of chronically implanted probes have been extensively investigated in the past few years [1][2]. One of the major limitations is the diminishing ability of the implanted probe to record over sustained periods of time. It is believed that the formation of an increased layer of glial cells (gliosis) that develops in the proximity of the electrode sites has a major role in obscuring the signals of interest [3].

Traditionally, the number of isolated single units in addition to the SNR have been used to quantify the degree of encapsulation [4]. A decrease in the number of units and/or the SNR is almost always accompanied by an increase in the electrode impedance. Both indicate a possible increase in the "insulating sheath" caused by the tissue response to the implanted device, which typically spans a range of 10-200 μm [2]. The use of electrode impedance to quantify the encapsulation process stems from modeling the electrochemical properties of the tissue with an equivalent circuit model to match the Electrochemical Impedance Spectroscopy (EIS) data measured[5]. In the EIS method, the measured impedance data is fitted to an equivalent circuit model using analog circuit components using a non-linear least squares algorithm [6]. The objective is to find the model parameters that cause the best agreement between the model's impedance spectrum and the measured spectrum.

Generally speaking, the equivalent circuit model has some limitations. First, the model is not unique [5], i.e. multiple circuits can yield the same impedance data. Second, the spatial resolution is severely limited, i.e., it is assumed that the same structure of encapsulation tissue exists at each electrode interface. While this may be true to a first order approximation, it does not capture the dynamics of the buildup process over time, save that fitting every electrode impedance data is cumbersome, especially with a high-density electrode array. Third, there is an inherent difficulty in achieving a steady-state of the system being measured. In particular, the EIS technique is a lengthy process during which the interface may have considerably changed. Fourth, the iterative and computationally complex nature of the associated fitting algorithms, their susceptibility to noise, and poor model fit make them impractical.

An alternative approach is to model the electrode tissue interface with Finite Element Model (FEM) to characterize the current flow in the surrounding tissue by solving Laplace voltage gradient equation [7]. Such models assume isotropic properties of the tissue. This assumption may be inaccurate because as the amount of encapsulation grows, anisotropic tissue properties arise. In addition, the distortion in the extracellular field due to the substrate presence causes directivity patterns that do not yield an ultimate recording configuration [8].

In this paper, we propose a different approach to quantify and track the degree of encapsulation. The approach is fully data-driven, in the sense that it uses systems theory to model the interface as a time varying communication channel. In addition, it is best suited for high-density electrode arrays since it does not make any assumptions about the tissue properties, nor the probe substrate design. Contrary to the EIS technique which is based on applying an AC voltage to the electrode and measuring the resulting current, the channel is modeled as a Multi-Input Multi-Output (MIMO) system. Herein, the multi-inputs consist of the neural signal sources adjacent to the electrode array that contribute to the neural data, while the multi-outputs consist

Manuscript received April 3, 2006. This work was supported in part by NIH grant # NS047516-01A2.K. G. Oweiss is with the ECE Dept., Michigan State University, East Lansing, MI 48824 USA (Phone: 517-432-8137; fax: 517-353-1980; e-mail: koweiss@msu.edu).

of the electrode array measurements. The potential of such method is to avoid the above mentioned limitations of the EIS based methods by inferring an alternate set of parameters that dynamically track the encapsulation process at various stages of the implantation in the absence of any external input.

II. Theory

A. Data Model

It is assumed that an array of *M* electrodes measures the activity of *P* signal sources in a time interval of length *N*. at any given time instant *n*, the observations $\boldsymbol{y} \in \Re^{Mx1}$ represent a mixture of signal sources $\boldsymbol{s} \in \Re^{P\times 1}$ and a zero mean additive noise component $\boldsymbol{z} \in \Re^{Mx1}$ according to the model

$$\begin{aligned} \boldsymbol{y}[n] &= \boldsymbol{A}_n \boldsymbol{s}[n] + \boldsymbol{z}[n] \\ &= \boldsymbol{x}[n] + \boldsymbol{z}[n] \end{aligned} \qquad n = 0,\ldots,N-1 \tag{1}$$

where $\boldsymbol{A}_n \in C^{M\times P}$ is the complex channel matrix at time *n*. Though it is known that electrochemical systems are nonlinear, a pseudo-linear response is obtained with the EIS method if the current range used is relatively small, which can circumvent the problem by linearizing the Butler–Volmer equation [5]. We therefore assume our data model is within that same range of operation.

From a MIMO system viewpoint, the channel matrix $\boldsymbol{A}_n$ models all the temporal and spatial characteristics of the channel at any given time *n*. We note that the channel model captures both the variable encapsulation layer structure as well as any frequency-dependent phase element (such as the purely-capacitive electrode effect [9]) in the $M \times P$ coefficient matrix $\boldsymbol{A}_n$. Temporal variations are captured by simply indexing each of these matrix entries by the array snapshot index *n*.

B. Channel Spatio-Temporal Characteristics

There is a plethora of techniques from systems theory that can be used to estimate the time-varying parameters of the channel matrix as well as accurately describe their correlation over time [11]. For example, the $M \times P$ parameters can be reduced to a $P \times P$ parameter set by simply factoring $\boldsymbol{A}_n = \boldsymbol{Q}\boldsymbol{H}_n^T$ [11]. The $M \times P$ matrix $\boldsymbol{Q}$ is popularly known to correspond to a spatial *whitening* matrix that can be determined from the data at $n = 0,\ldots,N-1$. This matrix captures all the spatial characteristics of the channel and therefore permits spatial resolution to be achieved. The matrix $\boldsymbol{H}_n$, on the other hand, is known to be a $P \times P$ unitary *rotation* matrix on the space $C^{P\times 1}$ and describes the temporal variation (often degradation) of the *P* signal sources present in the data [11].

C. Channel Estimation with Orthogonal Transformation

Quantifying the temporal changes that may occur to the encapsulation layer using the neural data is feasible by further examining the effect of the matrix $\boldsymbol{H}_n$. The rotation introduced by $\boldsymbol{H}_n$ can cause the signals to fade away if the $P \times N$ signal matrix $\boldsymbol{S} = [\boldsymbol{s}_1 \ \boldsymbol{s}_2 \ \ldots \ \boldsymbol{s}_P]^T$ is rotated in a direction where the "neural noise" dominates [13]. This correlates with the observation that not *every* electrode suffers from the same degree of encapsulation [6], and therefore variable SNR is observed across the array elements. Therefore, a key element to be able to track the channel relies on "undoing" this rotation.

Classically, $\boldsymbol{H}_n$ can be optimally determined using a variety of methods using training (pilot) signals. These can be a sequence of "microstimulation-like" signals (known $\boldsymbol{S}$) to *probe* the channel using a subset of the electrodes. In the latter case, they have to be chosen to satisfy certain orthogonality conditions [11]. Clearly, this is not a viable way in a neural tissue environment, though pilot signals can be designed adequately to avoid any adverse effects. An alternative is to "null" the effect of $\boldsymbol{H}_n$ on the signal matrix $\boldsymbol{S}$. The key in this step is to find a suitable matrix such that the signals can be continuously *strengthened* with respect to the "noise" over time. An important consideration is to avoid altering the span of the signal subspace (columns of $\boldsymbol{A}_n$) during this nulling process for the signals to remain intact.

For reasons that are beyond the scope of this paper [15], we opted to use an orthogonal basis set that projects the data matrix onto a set of nested multiresolution spaces. This can be efficiently achieved using a discrete wavelet transformation (DWT). This can be justified by noting that the DWT orthogonal transformation is known to introduce a substantial degree of sparseness in the transformed data. Let's denote by $\boldsymbol{W}^{(j)}$ a $N \times N$ DWT orthogonal transformation operator at subband *j*, where $j = 0, 1, \ldots, J$. Let's operate on the noise-free data matrix in (1) to obtain

$$\begin{aligned} \boldsymbol{X}_j &= \boldsymbol{A}_n \boldsymbol{S}\boldsymbol{W}^{(j)} \\ &= \boldsymbol{Q}\boldsymbol{H}_n^T \boldsymbol{S}\boldsymbol{W}^{(j)} = \boldsymbol{Q}\boldsymbol{H}_n^T \boldsymbol{S}_j \end{aligned} \qquad j = 0,1,\ldots,J \tag{2}$$

where $\boldsymbol{S}_j$ denotes the signal matrix projected onto the span of wavelet basis $\phi_{j,k} = 2^{j/2}\phi(2^j . - k)$. To null the effect of $\boldsymbol{H}_n$ in subband *j*, or equivalently separate the signal components in $\boldsymbol{X}_j$, we perform spectral factorization of (2) using Singular Value Decomposition (SVD) to yield

$$\boldsymbol{X}_j = \boldsymbol{U}_X^j \boldsymbol{D}_X^j \boldsymbol{V}_X^{jT} \quad (3)$$

From this factorization, it is known that the columns of the eigenvector matrix $\boldsymbol{V}_X^j$ span the row space of $\boldsymbol{X}_j$, i.e., the space spanned by the transformed signals $\boldsymbol{s}_p^j$, $p = 1,...,P$, which are now sparse. This means that $\boldsymbol{s}_p^j$ will have a few entries that are nonzero. This property enables us to infer a relationship between the row space of $\boldsymbol{X}_j$ and that of $\boldsymbol{X}$. Specifically, by comparing (2) and (3) and noting that when $\boldsymbol{W}^{(j)}$ spans the *null* space of the matrix $\boldsymbol{H}_n^T \boldsymbol{S}$, the corresponding rows of $\boldsymbol{H}_n^T \boldsymbol{S}_j$ will be zero. Conversely, if $\boldsymbol{W}^{(j)}$ spans the *range* space of $\boldsymbol{H}_n^T \boldsymbol{S}$, then the corresponding rows of $\boldsymbol{H}_n^T \boldsymbol{S}_j$ will be nonzero. Furthermore, they will belong to the subspace spanned by the columns of the whitening matrix $\boldsymbol{Q}$.

Given the spectral factorization of $\boldsymbol{X}_j$ in (3), a necessary (but not sufficient) condition for a column of $\boldsymbol{V}_X^j$ to span the row space of $\boldsymbol{X}_j$ is the existence of at least one row of $\boldsymbol{H}_n^T \boldsymbol{S}_j$ that is nonzero. If such a row exist, then a corresponding column in $\boldsymbol{Q}$ will be obtained, which is equivalent to test the columns of $\boldsymbol{U}_X^j$. This argument elucidates that any perturbation in the number of linearly independent eigenvectors in $\boldsymbol{V}_X^j$, or equivalently the number of distinct eigenvalues in $\boldsymbol{D}_X^j$, is directly reflected in the corresponding columns of $\boldsymbol{U}_X^j$.

D. Invariance of the Number of Neurons

The above analysis is based on two important observations: *First*, the number of signals that can be reliably estimated does not change over the period of the encapsulation layer buildup aside from adverse factors such as neuronal cell death. This statement is reinforced by the observation that "rejuvenation" achieved by biasing the electrodes occasionally restores the signals [6]. If the appropriate subbands where $\boldsymbol{H}_n^T \boldsymbol{S}_j$ is nonzero can be identified, then the channel is effectively *equalized,* and the nulling effect is termed "positive". These subbands are the ones for which the *P* diagonal entries in $\boldsymbol{D}_X^j$ are "large" enough compared to the remaining *M-P* entries. *Second*, any degradation of the signals over time will result in: 1) a gradual decrease in signal energy in a subset of subbands where the wavelet basis best approximates the *original* signals and, 2) an energy increase in other subbands where the degraded signals are best matched by the wavelet basis. This is because the wavelet operators in adjacent subbands approximate the signal matrix in a complementary fashion.

III. Methods

We simulated the observed deterioration of the signals using the impedance of an equivalent circuit model of the encapsulation layer shown in Figure 1. We used template spike waveforms from recording archives (Figure 2). Thus the signals at the input of the channel were known. We varied the model parameter accounting for tissue resistance R_{ex} (low frequency circuit pathway) in a continuous fashion to mimic the incremental build-up of the resistive component of the encapsulation layer on one electrode. We repeated the same synthesis for a total of 16 electrodes with variable increments of R_{ex}. Table I summarizes the settings for the other parameters.

From the above synthesis of attenuated signals, a MIMO model was developed to observe the corresponding change in the model parameters. We observed these changes over the period in which 100 spike events occurred and quantified the changes in channel parameters as estimated from equation (3) relative to the first event.

TABLE I
PARAMETERS FOR EQUIVALENT CIRCUIT MODEL OF THE NEURAL INTERFACE

Element	Value
C_m	10^{-6} uF/cm^2
R_m	3.33 Ω/cm^2
R_{ex}	1 MΩ/cm^2-10 MΩ/cm^2
R_Ω	1 kΩ

IV. Results

Figure 3 illustrates the percentage changes in the spectro-temporal energy of the signals relative to the first event. It is clearly seen that the dynamics of the channel are efficiently captured by the model parameters across a subset of the wavelet subbands. Some subbands exhibit a decrease in signal energy corresponding to those channel parameters characterizing increased tissue impedance. On the other hand, the subset of subbands in which the projected signal energy has increased implies that these subbands are the best ones to *equalize* the channel. An example of a neural trace from the Dorsal Cochlear Nucleus of an adult guinea-pig is illustrated in Figure 4 for an encapsulated electrode. The result of equalizing the channel is also illustrated to show the substantial improvement in SNR.

V. Conclusion

The formation of reactive tissue on chronic implants is a problem for which a solution is of fundamental importance to the longevity and viability of implantable neuroprosthetic devices. This study shows that characterizing the electrode-tissue interface in terms of systems theory enables better quantification of the parameters of the encapsulation layer. Signals can be adequately "pulled out of noise" by equalizing the channel and enable better characterization of the progression of the encapsulation process in quantitative terms. It overcomes shortcomings of FEM and EIS that assume tissue isotropic properties and regularity of glial scar structure on each electrode. The method can substantially be used to quantify the degree of gain and/or loss of signals over long periods of time. Potential microprobing signals can be adequately designed and used to probe the time varying channel if adverse effects can be neglected.

References

[1] J. C. Williams, R. L. Rennaker, and D. R. Kipke, "Long-term neural recording characteristics of wire microelectrode arrays implanted in cerebral cortex," *Brain Res. Protoc.*, vol. 4, pp. 303–313, 1999.

[2] A. B Schwartz, "Cortical Neural Prosthetics," Annu. Rev. Neurosci. 2004.27:487-507.

[3] X. Liu, D. B. McCreery, R. R. Carter, L. A. Bullara, T. G. Yuen, andW. F. Agnew, "Stability of the interface between neural tissue and chronically implanted intracortical microelectrodes," *IEEE Trans. Rehabil Eng.*, vol. 7, no. 3, pp. 315–326, Sep. 1999.

[4] D. H. Szarowski, *et al.*, "Brain responses to micromachined silicon devices," *Brain Res.*, vol. 983, pp. 23–35, 2003.

[5] *Impedance Spectroscopy; Theory, Experiment, and Applications, 2nd ed.* , E. Barsoukov, J.R. Macdonald, eds., Wiley Interscience Publications, 2005.

[6] K. Otto, M. Johnson, D. Kipke, "Voltage Pulses Change Neural Interface Properties and Improve Unit Recordings With Chronically Implanted Microelectrodes," IEEE Trans. on BME, pp. 333-340, Feb 2006

[7] K. G. Oweiss, M.K. Wise, C. Lopez, J. Wiler, and D.J. Anderson, "Chronic Electrode-Brain Interface Modeled with FEM," Proc. of IEEE- EMBS, pp. 453, vol.1, 1999

[8] K. G. Oweiss, D.J. Anderson, "Neural Source Localization using Advanced Sensor Array Signal Processing Techniques," Proc. of 23rd IEEE EMBS, pp. 707-710, October 2001

[9] J. D.Weiland and D. J. Anderson, "Chronic neural stimulation with thin film, iridium oxide electrodes," *IEEE Trans. Biomed. Eng.*, vol. 47, no. 7, pp. 911–918, Jul. 2000.

[10] K. G. Oweiss, " Source Detection in Correlated Multichannel Signal and Noise Fields," Proc. of ICASSP, vol.V, pp. 257-260, Hong Kong , April 2003

[11] A. Jagannatham and B. rao, "Whitening-Rotation-Based Semi-Blind MIMO Channel Estimation," IEEE Trans. on SP, pp. 861-870, March 2006

[12] K. Wise *et. al.*, **"**Wireless Implantable Microsystems: High-Density Electronic Interfaces to the Nervous System," *Proc. of the IEEE*, Vol.: 92-1, pp: 76–97, Jan. 2004

[13] K. Oweiss, D. Anderson, "Tracking Signal Subspace Invariance for Blind Separation and Classification of Non-orthogonal Sources in Correlated Noise" *EURASIP journal on Applied Signal Processing*, 2006, in press.

[14] K. G. Oweiss, D.J. Anderson, "Neural Channel Identification of Multichannel Neural Recordings Using Multiresolution Analysis," Annals of the 22nd Biomedical Engineering Soc., 28 (Suppl. 1): p. S-116, 2000

[15] K. G. Oweiss, "A Systems Approach for Data Compression and Latency Reduction in Cortically Controlled Brain Machine Interfaces," *IEEE Transactions on Biomedical Engineering,* vol. 53, no.7, pp. 1364 – 1377, July 2006

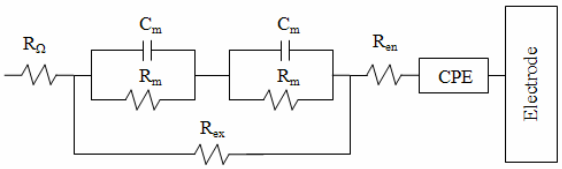

Figure 1: (a) One possible equivalent circuit model of the electrode-tissue interface [6]. CPE denotes a constant phase term modeling the capacitive effect of the electrode site.

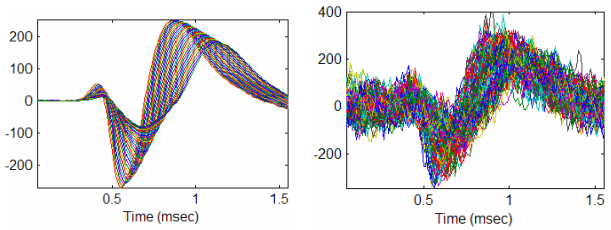

Figure 2: (Left) Template neural signal passed through an equivalent circuit model at 1 kHz with variable R_{ex} to mimic long-term impedance increase in chronic recording. The first event has the largest SNR. (Right): Noisy signals in left panel.

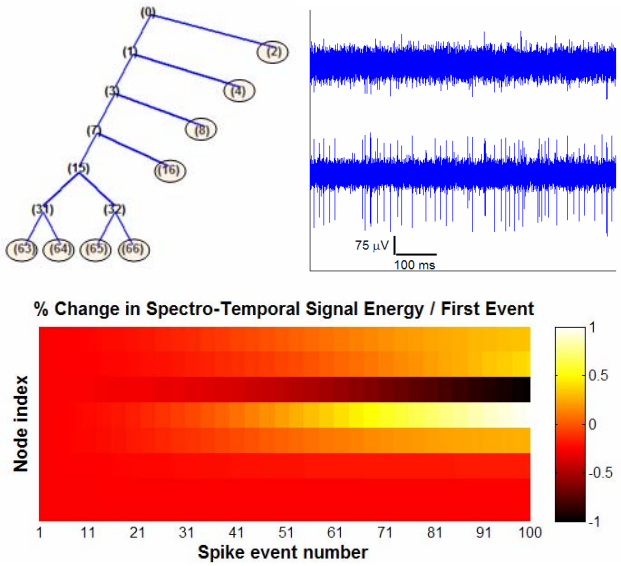

Figure 3: (a) Wavelet subbands characterizing changes in the channel parameters. (b) Example neural recording before channel equalization (top) and after channel equalization (bottom).
(c) Percentage change in signal energy in wavelet subbands relative to the first event for the signals in Figure 2. Node index represents the selected set of subbands where changes have been observed.